

**ISCI, Volume 21**

**Supplemental Information**

**Spoof Plasmonic Metasurfaces with Catenary**

**Dispersion for Two-Dimensional**

**Wide-Angle Focusing and Imaging**

**Yinghui Guo, Zuojun Zhang, Mingbo Pu, Yijia Huang, Xiong Li, Xiaoliang Ma, Mingfeng Xu, and Xiangang Luo**

### Supplemental Figures

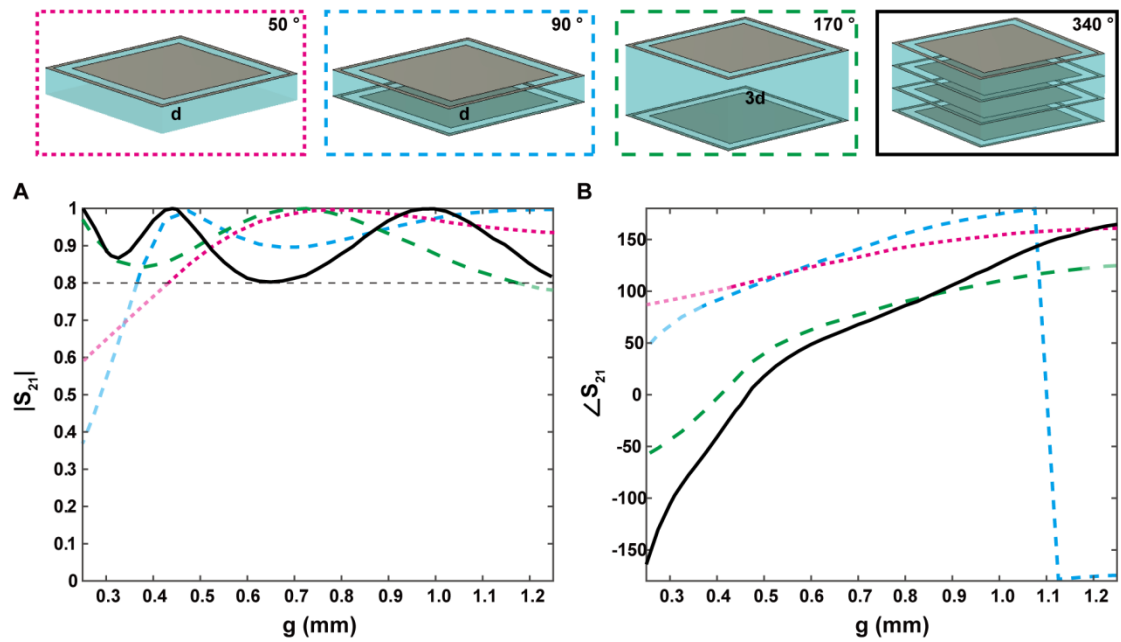


Figure S1. Simulated (A) amplitude and (B) phase of  $S_{21}$  at 30 GHz changing with the slit width for different configurations shown in the top. The black curve represents the design adopted in the proposed spoof metasurfaces. The achieved phase shift with transmission coefficient higher than 0.8 is respectively  $50^\circ$ ,  $90^\circ$ ,  $170^\circ$ , and  $340^\circ$ . Related to Figure 3F and 3G.

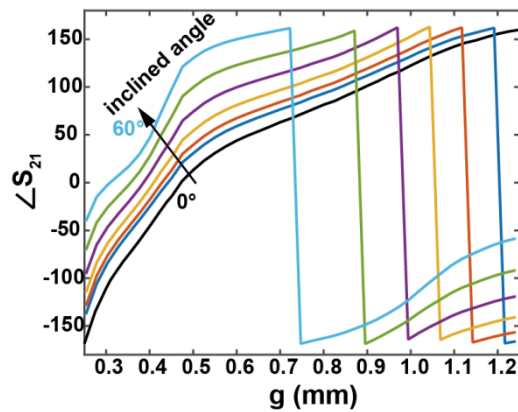


Figure S2. Simulated phase of  $S_{21}$  at 30 GHz changing with the slit width under different inclined angles. Related to Figure 3G.

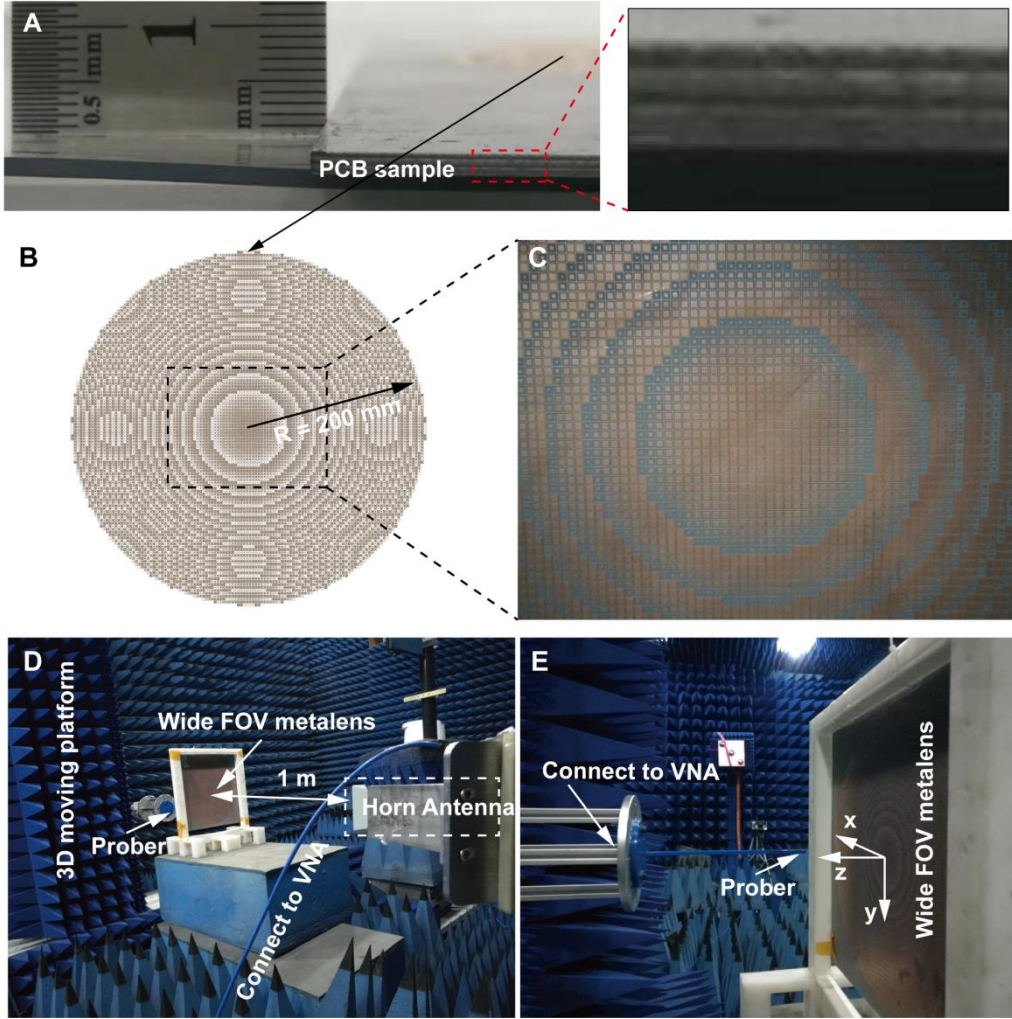


Figure S3. (A) A cross-view of the fabricated spoof plasmonic metalens. (B) A schematic of the proposed wide FOV spoof plasmon metalens. (C) Photography of a part of the fabricated metalens sample. (D) and (E) Photography of the measurement setup. Related to Figure 4A-L.

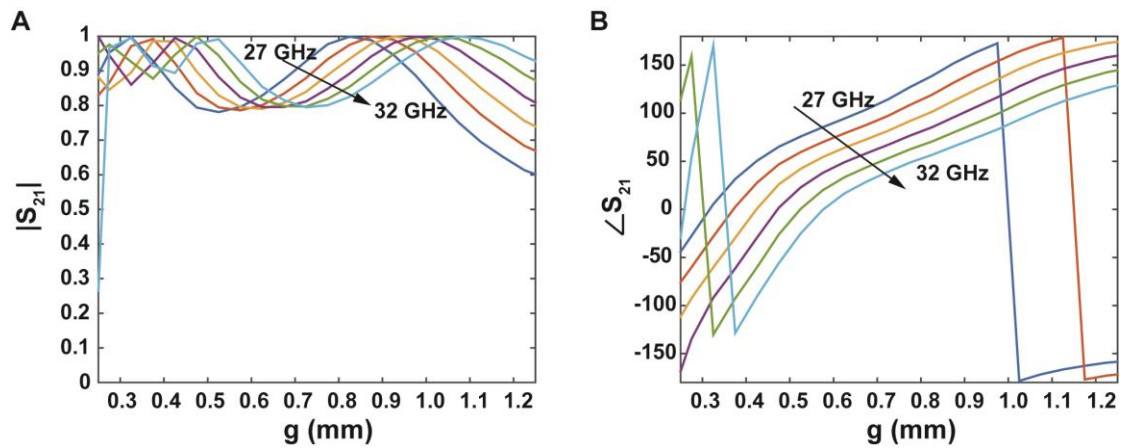


Figure S4. Simulated (A) amplitudes and (B) phases of  $S_{21}$  at different frequencies change with the gap width. Related to Figure 4A-L.

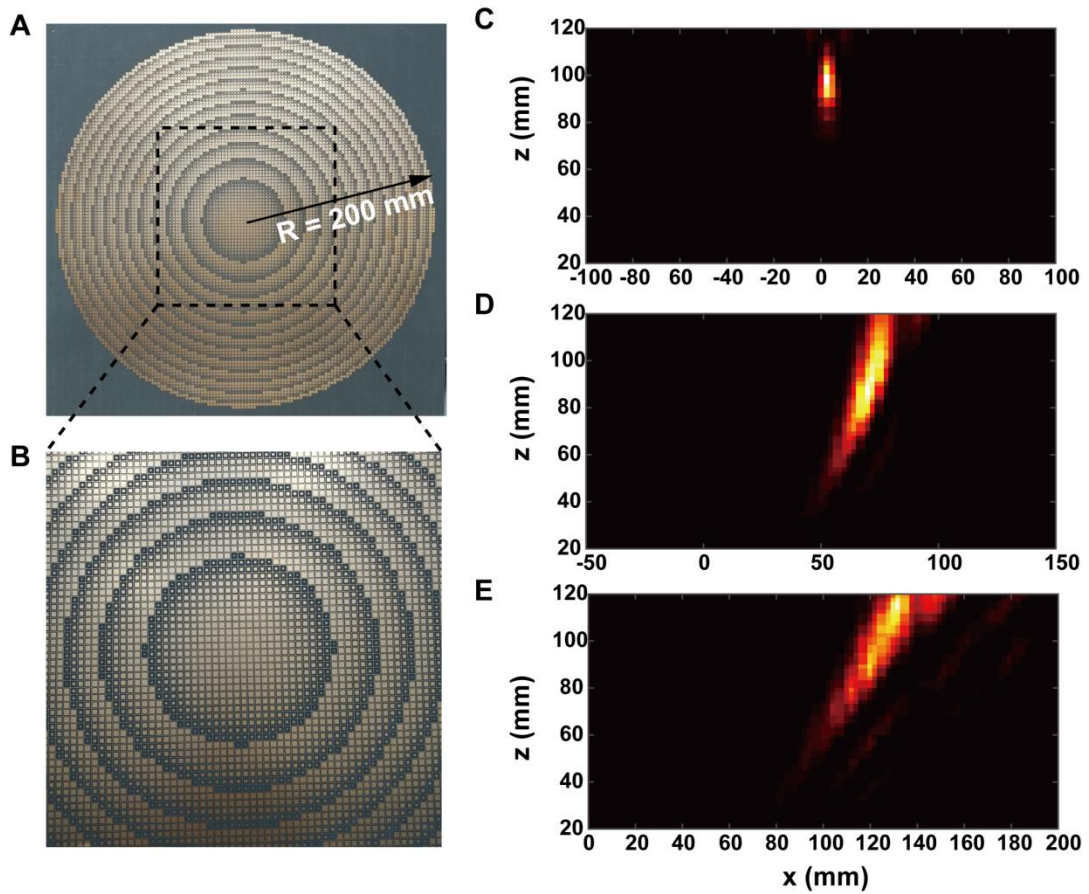


Figure S5. (A) (B) Photography the fabricated metalens sample with a spherical phase profile. (C)-(E) Measured intensity distribution along the  $xoz$  plane under different incidence angles of  $0^\circ$ ,  $30^\circ$ , and  $60^\circ$ . Related to Figure 5A, 5C, and 5E.

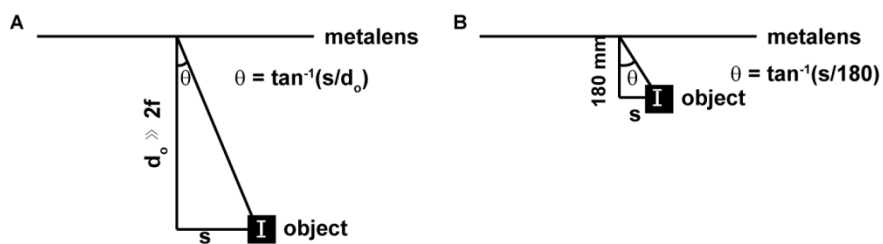


Figure S6. (A) Ideal and (B) practical characterization method of the FOV ( $2\theta$ ) of a metalens. Related to Figure 6A.

## Transparent Methods

### 1. Transfer matrix at the interface of metasurface

According to the continuous boundary conditions, the following equations can be established around the thin metallic patterns:

$$\begin{aligned} a + b &= c + d \\ Y_0(a - b) &= Y_d(c - d) + Y_{meta}(c + d) \end{aligned} \quad (1)$$

The equations above can be transformed into the matrix form:

$$\begin{aligned} \begin{bmatrix} a \\ b \end{bmatrix} &= M \cdot \begin{bmatrix} c \\ d \end{bmatrix} \\ &= \frac{1}{2Y_0} \cdot \begin{bmatrix} Y_0 + Y_{meta} + Y_d & Y_0 + Y_{meta} - Y_d \\ Y_0 - Y_{meta} - Y_d & Y_0 - Y_{meta} + Y_d \end{bmatrix} \cdot \begin{bmatrix} c \\ d \end{bmatrix} \end{aligned} \quad (2)$$

and in the dielectric substrate there is,

$$\begin{aligned} \begin{bmatrix} c \\ d \end{bmatrix} &= N \cdot \begin{bmatrix} e \\ f \end{bmatrix} \\ &= \begin{bmatrix} \exp(in_i k_0 d) & 0 \\ 0 & \exp(-in_i k_0 d) \end{bmatrix} \cdot \begin{bmatrix} e \\ f \end{bmatrix} \end{aligned} \quad (3)$$

Therefore, the whole transfer matrix of the proposed spoof plasmonic metasurface can be expressed as,

$$\begin{aligned} T &= (M \cdot N)^3 \cdot M \\ &= \begin{bmatrix} \frac{Y_0 + Y_{meta} + Y_d}{2Y_0} & \frac{Y_0 + Y_{meta} - Y_d}{2Y_0} \\ \frac{Y_0 - Y_{meta} - Y_d}{2Y_0} & \frac{Y_0 - Y_{meta} + Y_d}{2Y_0} \end{bmatrix} \begin{bmatrix} \exp(in_i k_0 d) & 0 \\ 0 & \exp(-in_i k_0 d) \end{bmatrix} \\ &\quad \left\{ \begin{bmatrix} 1 + \frac{Y_{meta}}{2Y_d} & \frac{Y_{meta}}{2Y_d} \\ -\frac{Y_{meta}}{2Y_d} & 1 - \frac{Y_{meta}}{2Y_d} \end{bmatrix} \begin{bmatrix} \exp(in_i k_0 d) & 0 \\ 0 & \exp(-in_i k_0 d) \end{bmatrix} \right\}^2 \begin{bmatrix} \frac{Y_d + Y_{meta} + Y_0}{2Y_d} & \frac{Y_d + Y_{meta} - Y_0}{2Y_d} \\ \frac{Y_d - Y_{meta} - Y_0}{2Y_d} & \frac{Y_d - Y_{meta} + Y_0}{2Y_d} \end{bmatrix}, \end{aligned} \quad (4)$$

### 2. Near-field scanning measurements

The setup of near-field scanning measurements in an anechoic chamber is shown in Figure S3(d) and (e). A linearly polarized horn antenna with the operation frequency from 26.5 to 40 GHz is connected to one port of a vector network analyzer (VNA) as the electromagnetic emitter, which is located about 1 m away from the metalens sample to ensure approximate plane wave incidence. A rectangular waveguide port with the same operation frequency with the horn antenna is connected to the other port of the VNA as the probe, which is fixed on the automatic test platform to achieve point-to-point scanning of the transmitted field. The fabricated metalens sample is fixed at a square frame and the antenna is fastened on a camera tripod. The center of the horn antenna, metalens, and the scanning area of the waveguide probe are aligned before measurement to decrease the influence of imperfect plane wave emitted from

the horn antenna. The alignment can be easily done by adjusting the height and position of the camera tripod and automatic test platform and checked the symmetry of the measured wavefront. The maximum scanning volume of the automatic test platform was 2800 mm × 2100 mm × 400 mm, satisfying the requirement of our measurement. A software in the control computer connected to the VNA and automatic test platform via a network interface provides the remote control. In the user interface of the software, we can assign the scanning manner according to the practical measurement requirement, including the starting position and orientation of waveguide probe, sampling interval, sampling points number, scanning velocity, horizontal scanning, vertical scanning and two dimensional scanning. During the scanning process, the waveguide probe will scan across these pre-assigned positions and the vectorial transmitted field including the amplitude and phase at each scanning point can be measured by the VNA. Finally, the measured results can be recorded and displayed by the software in the control computer or exported for post-processing.